2000 유체기계 연구개발 발표회 논문집, pp. 325~333
부경대학교 용당캠퍼스 종합복지관, 2000. 12. 1~2.

파력 발전용 웰즈터빈의 유동특성에 관한수치적 연구

이형구* · 김정환** · 이연원***

Numerical Analysis of Flow Characteristics in the Wells Turbine for Wave Power Conversion

Hyeong-Gu Lee, Jeong-Hwan Kim, , Yeon-Won Lee

Key Words: Wells Turbine(웰즈터빈), Wave Power Conversion(파력발전), Natural Energy(자연에너지), Ocean Energy(해양에너지), Fluid Machinery(유체기계), Angle of Attack(영각), Steady Flow(정상상태)

ABSTRACT

The aerodynamics of the Wells turbine has been studied using a 3-dimensional, unstructured mesh flow solver for the Reynolds-averaged Navier-Stokes equations. The basic feature of the Wells turbine is that even though the cyclic airflow produces oscillating axial forces on the airfoil blades, the tangential force on the rotor is always in the same direction. Geometry used to define the 3-dimensional numerical grid is based upon that of an experimental test rig. The 3-dimensional Wells turbine model, consisting of approximate 220,000 cells is tested at four axial flow rates. In the calculations the angle of attack has been varied between 10° and 30° of blades. Representative results from each case are presented graphically and analyzed. It is concluded that this method holds much promise for future development of Wells turbines.

1. Introduction

Much attention in recent years has been focused on the availability of natural or renewable energy because of environmental damage and for the purpose of energy replacement. Many ocean energies such as wave, tide, wind and solar energy etc. especially potential wave power is useful and economic. A number of prototype wave power plants have already been in operation in Japan, England and Norway, which have plenty ofwave power sources. There are technical difficulties such as power change and installation problem of a great power plant on the sea for the purpose of wave energy generation, but we expect that in the beginning of year 2000 it is possible to generate great wave power.

The fixed prototype of wave power plant was operated in Kaimei, Japan(240 KW power) and JAMSTEC proceeded to install a buoyancy type of wave power plant(540 KW power). A wave power plant is being driven in Queen's university of Belfast, United Kingdom(75 KW power).

Wave power plants in Norway and Denmark are going to be constructed.[2] And wave energy is very attractive natural energy in consideration of geographic characteristics of the Republic of Korea which has long coastlines.

* 부경대학교 대학원
** 부경대학교 대학원
(현 한국해양대학교 박사과정)
*** 부경대학교 기계공학부

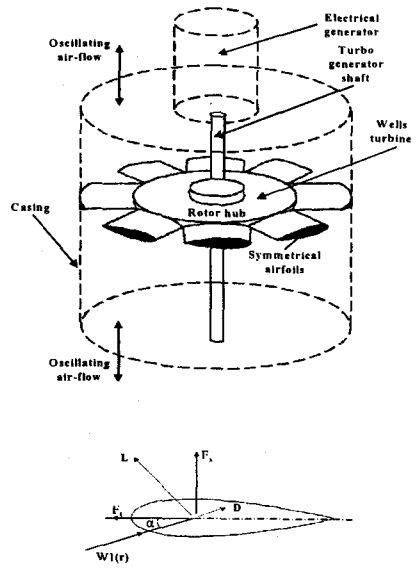

Fig. 1 Schematic of Wells turbine

Wells turbine is a self-rectifying air turbine, which is most widely used and one of the most successful method of achieving wave power with use of the principle of an OWC(oscillating water column.[3]

This ells turbine consists of uncambered airfoil blades with constant solidity around the axis as shown in Fig. 1.

Since the turbine is symmetric about its central plane and blades are set normal to the axis of rotation, it is capable of uni-directional rotation, while operating in a bi-directional airflow. The investigation through numerical simulations of a Wells turbine dependent upon angles of attack is presented by Suzuki.[7] In Suzuki's paper numerical simulation is performed under the conditions of the laminar flow and 19° and 30° angles of attack. In our paper it is accomplished under the conditions of the turbulence flow and angles of attack between 1 0° and 30° .We examined the flow characteristics dependent upon various angles of attack. in this paper we tried to make "flow model" of several experimental data in the Wells turbine with use of CFD code. It was very difficult for us to model this work due to Wells turbine's peculiar geometry which has complex flow patterns and demands very fine grid generation. First we have analyzed 2-dimensional, steady and incompressible airflow around an uncambered blade in the test rig of the Wells turbine, and them we have modelled and calculated 3-dimensional Wells turbine's geometry.

2.Computational conditions

2.1 Numerical analysis code

We have chosen FLUENT[4] as a CFD-code, because it has a large number of modelling capability regardless of complex geometry.

The continuity and momentum equations are discretized with a FVM(Finite Volume Method) and solved with the SIMPLE algorithm 10. Grids are generated in a single block.

2.2 Computational conditions of 3-D Wells turbine

Our computation model is based on the Wells turbine's experimental data of Suzuki.[8] The Wells turbine which has 8 airfoil blades with high solidity of 0.72 and tip clearance of 2 mm is set in a cylindrical duct. Air in chamber is sucked from a bell-shaped suction port and delivered through a turbine to the outlet. A number of simplifications were made on the generation of 3-D grid. Due to the rotationally cyclic nature of the turbine geometry and of the expected flow patterns, the region around one blade only was modelled and cyclic boundary conditions were applied (Fig. 2). It was calculated in comparison of many cases with angles of attack between 10° and 30° at constant flow rates. Fig. 3 shows grid distributions on the blade surface and around the surface. We has used unstructured mixed grids which consist of triangular meshed around the blade and rectangular meshed on the blade surface.

And the number of grids consists of 220,000

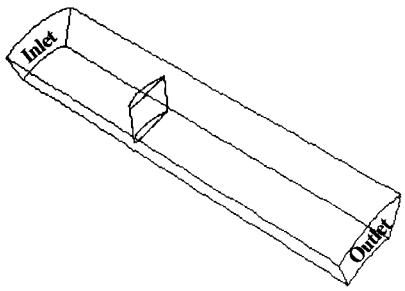

Fig. 2 Computational Domain

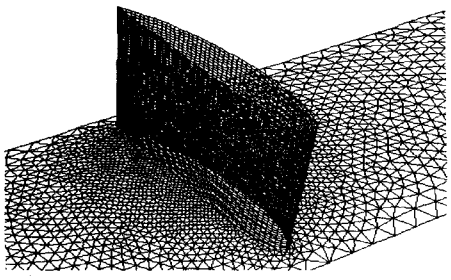

Fig. 3 3-Dimensional Grid of a Wells Turbine

meshes and the number of grids on the blade surface are 9,800. A RNG k-ε model as turbulent model is used and a QUICK scheme applied.

3. Analysis results and consideration

Figures 4 to 6 show the flow characteristics such as velocity vectors, streamlines and pressure distribution in the suction side under conditions of z=8 (number of blade), s=0.72 (solidity) and t=2mm (tip clearance) at angles of attack between 10° and 30° . Fig. 7 shows axial velocity vectors and uniform velocity distributions on the projected surface in the mid-chord plane of a blade.

Fig. 8 shows relative velocity on a grid plane of constant radius. Fig. 4 and Fig. 5 show that separation points move forward from the trailing

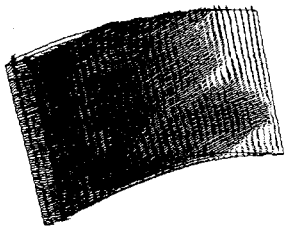

(a) angle of attack=10°

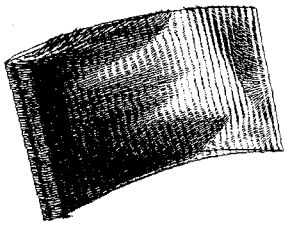

(b) angle of attack=20°

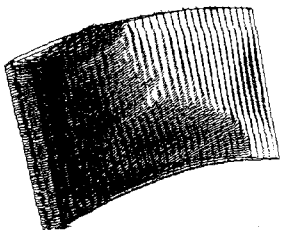

(c) angle of attack=25°

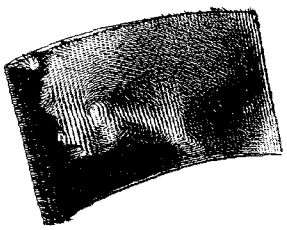

(d) angle of attack=30°

Fig. 4 Velocity vector on suction side

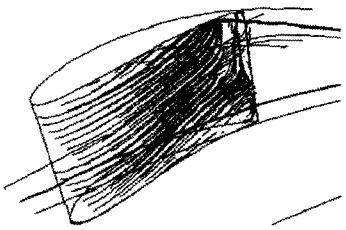

(a) angle of attack=10°

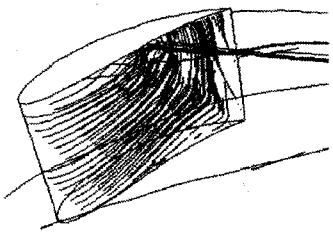

(b) angle of attack=20°

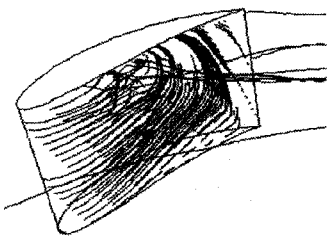

(c) angle of attack=25°

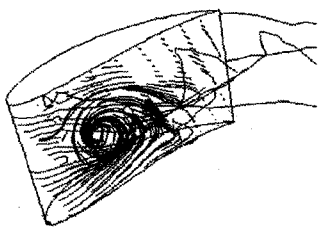

(d) angle of attack=30°

Fig. 5 Streamlines flowing over suction side

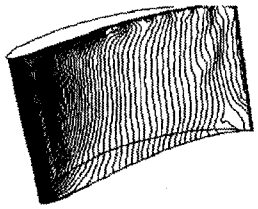

(a) angle of attack=10°

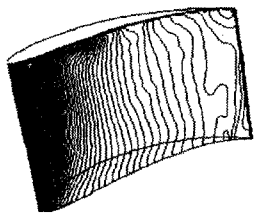

(b) angle of attack=20°

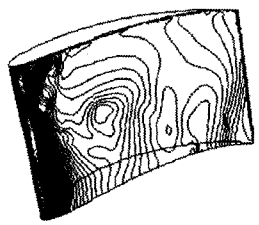

(c) angle of attack=30°

Fig. 6 Static pressure distributions on suction side

edge to the leading edge in the increasing process of angles of attack.

It is observed that the flow direction from the leading edge to the trailing edge starts to reverse and stall occurs from an angle of attack of 25° . It is apparent as shown in Fig. 6 due to these pressure distributions.

In consideration of these pressure distributions the minimum pressure is observed near the tip of a leading edge at a lower angle of attack, but the minimum pressure point moves to the hub as the angles of attack increases. And at a 30° of angle of attack vortex is observed in the central region over the suction side.

Fig. 7 shows velocity vectors and uniform

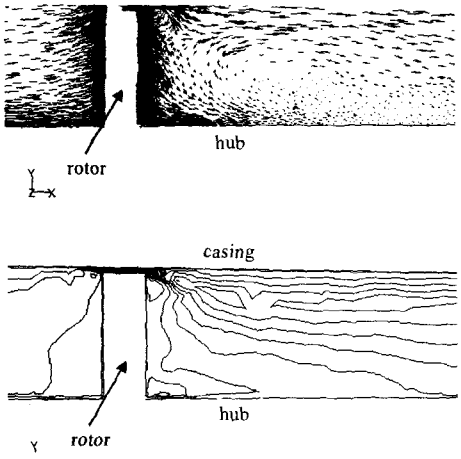

(a) angle of attack=10°

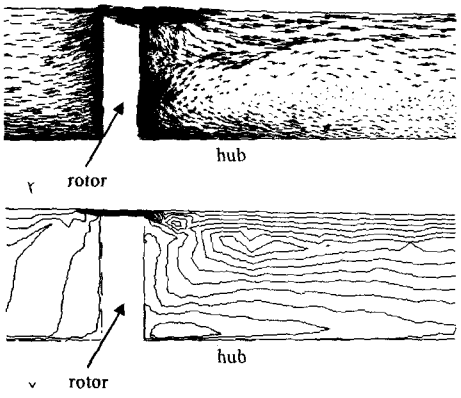

(b) angle of attack=20°

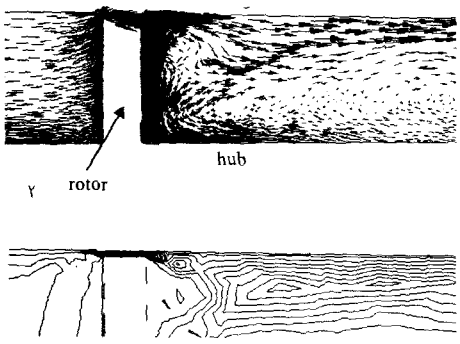

(c) angle of attack=30°

Fig. 7 Velocity vectors and x-direction distributions projected onto a meridional grid plane

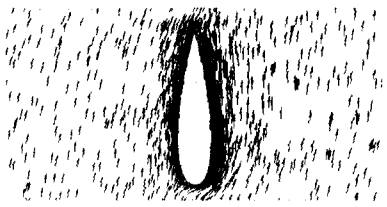

mid-span

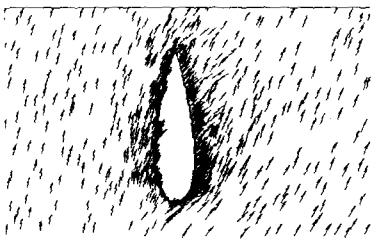

Just beneath tip

(a) angle of attack=10°

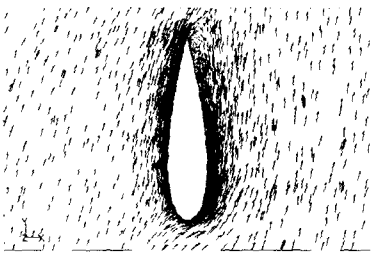

mid-span

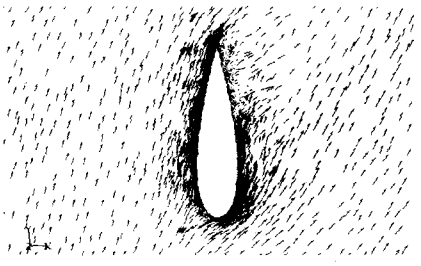

Just beneath tip

(b) angle of attack=15°

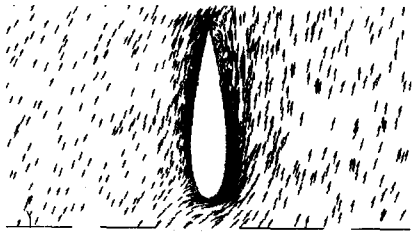

mid-span

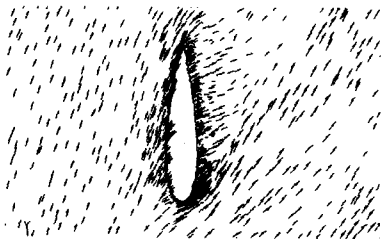

Just beneath tip
(c) angle of attack=20°

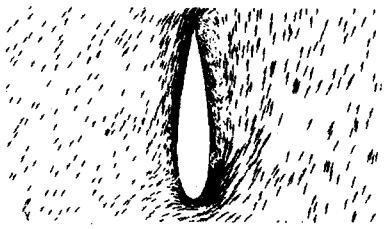

mid-span

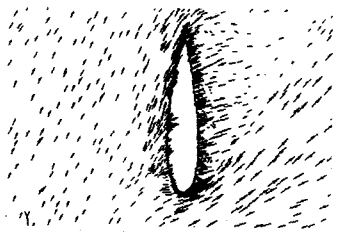

Just beneath tip
(d) angle of attack=30°

Fig. 8 Relative vectors contours on planes of constant radius

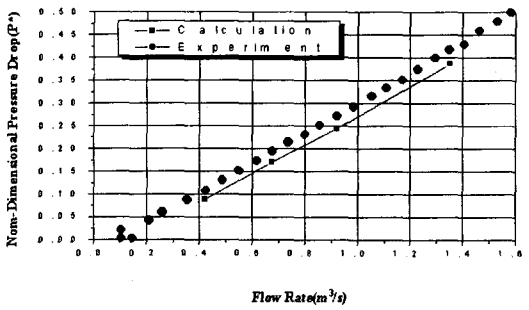

Fig. 9 Comparison of experimental and numerical pressure drops across the turbine

velocity distribution on the mid-chord plane of a blade. Also as an angle of attack increases, it is shown that unstable flow field is apparent and vortex near the casing of downstream of a blade grows up and vortex at the tip edge is increasing. Fig. 8 shows relative velocity vectors near the tip on constant hub radius at angles of attack between 10° and 30° . First at á=10° constant pressure distributions near the hub are apparent, but from á=15° vortex is observed to occur in the trailing edge of a blade and at á=30° vortex.

Because the velocity near tip is faster than near hub, vortex is being generated in the trailing edge of a blade from á= 10° . And it is observed that the magnitude of vortex is increasing and prevailing as an angle of attack increases.

Fig. 9 shows the comparison between numerical and experimental non-dimensional pressure drops across the turbine by Warfield12), 1994. At tip clearance of 1% the numerical results are found to be in good agreement with experimental data at each flow rate.

Figures 10 to 12 show velocity vectors, static pressure distributions and streamlines over suction side for various tip clearances at constant axial velocity and with rotational speed of 2,000 rpm of a Wells turbine.

Seperation is apparent in the wide range near the trailing edge of a blade and the radial flow increased along the trailing edge due to the

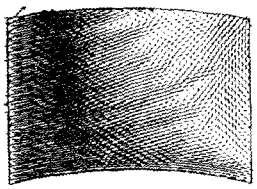

(a) tip clearance=0%

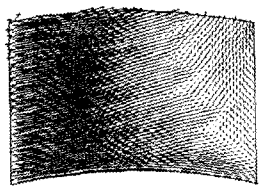

(b) tip clearance=2%

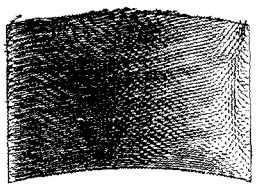

(c) tip clearance=6%

Fig. 10 Velocity vector on suction side

centrifugal force through rotation of a rotor as show in Fig. 10 (a).

As tip clearances increase , highest rotational speed is able to be apparent at blade tip, so that separation moves to the trailing edge due to increased momentum as seen in Fig. 10 (a) and (c).

We can see this in the streamlines of Fig.11, and due to this effect of tip flow, the pressure distributions over tip are affected as shown in Fig. 12 (a)~(b). Fig. 13 shows the coefficients of pressure drops with various tip clearance. As tip clearance increased, the coefficient of pressure drops decreased generally, but they are almost constant between 0% and 1% of tip clearance and they decreased greatly from tip clearance of 2%. This means that proper tip clearances are less than 1%

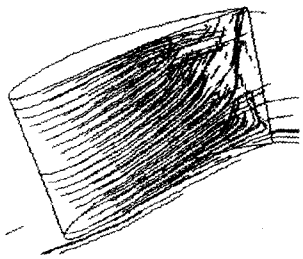

(a) tip clearance=0%

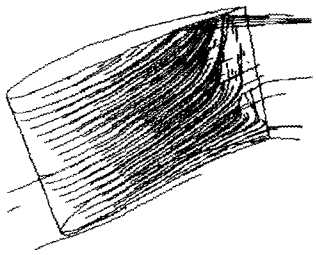

(b) tip clearance=2%

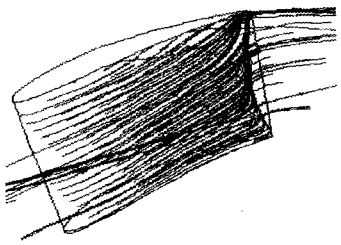

(c) tip clearance=6%

Fig. 11 Streamlines flowing over suction side

in consideration of a turbine's efficiency and we defined the coefficient of non-dimensional pressure drops as follows.

4. Conclusions

Through numerical analysis of flow characteristics in a Wells turbine for wave power conversion with the effects of angles of attack we have concluded as follows.

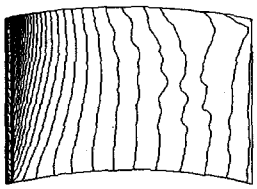

(a) tip clearance=0%

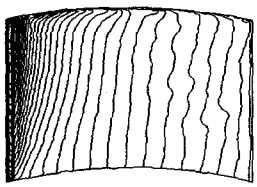

(b) tip clearance=2%

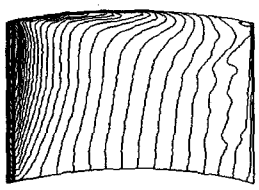

(c) tip clearance=6%

Fig. 12 Static pressure distributions on suction side

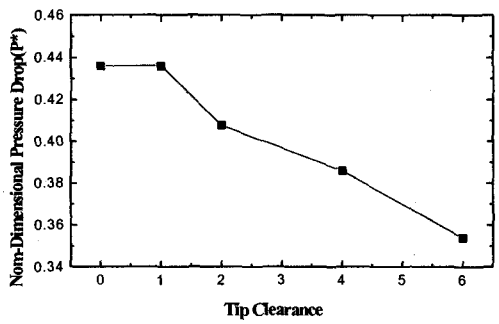

Fig. 13 Variation of pressure drop with clearance (ϕ=1.351)

1) From the lower to the upper angle of attack the airflow around the blade of a Wells turbine directs towards the tip, and from á= 25° the direction of airflow is toward the leading edge. And at á=30° very large vortex occurs in the central part of a blade, so from these results we need to develop a turbine which can rotate very fast also at small flow rates in order to control stall.
2) As tip clearance decreased, kinetic energy decreased due to viscous frictions near casing and hub, so that the ranges of re-circulations increased through inverse pressure gradient.
3) It is concluded that 0%<tip clearance≤1% is adequate in consideration of the efficiency and flow characteristics of a turbine through numerical simulation of a Wells turbine.

References

(1) A. Thakker., S. Slater., "A Study of CFD Airflow Predictions in A Wells Turbine" International Offshore and polar Engineering Conference May 24~29 1998.
(2) C. L. Ryu, "Ocean energy engineering" New technique, pp. 75~123.
(3) Falcao, A. F. O., Whittaker, T. J. T. and Lewis, A. W.(1993) JOULE II Preliminary Action: European Pilot Plant Study, Proc. 1993 European Wave Energy Symp., pp. 247~257.
(4) FLUENT Users Manuals, Fluent Inc.
(5) Harris, C. D., "Two-Dimensional Characteristics of the NACA0012 Airfoil in the Langley, 8-Foot Transonic Pressure Tunnel" NASA Technical Memorandum 1927, April 1981.
(6) L. M. C. Gato., A. F. de O. Falcao., "On the Theory of the Wells Turbine" Journal of Engineering for Gas Turbines and Power vol.106 pp. 628~633, 1984.
(7) M. Suzuki, C. Arakawa, Numerical Simulation of Flow around Wells Turbine for Wave Power Generator, (in Japanese), Procs. of 1999 JSME Annual Meeting (No.99-1), pp. 199~200,1999
(8) M. Suzuki, C. Arakawa, T. Tagori, Wells Turbine Flow the Rotating Blade for Wave Power Generator Journal of the Flow

Visualization Society of Japan, (in Japanese), Vol.4, Suppl. pp 51~56,1984.

(9) M. Takao, T. Setoguchi, K. Kaneko, M. Inoue, "A Wells Turbine with Guide Vanes for Wave Energy Conversion" The Fifth Asian International Conference on Fluid Machinery, pp. 511~518 v1011.1997.

(10) Patankar, S. V., "Numerical Heat Transfer and Fluid Flow" Hemisphere, Washington, D. C. 1980.

(11) Thompson. Joe. F., Warsi, Z. U. A Warsi, C. Wayne Mastin, 1985, "Numerical Grid Generation" Elsevier Science Publishing Co.

(12) Warfield, V., An Investigation into the performance of a High Solidity Wells Turbine for an Oscillating Water Column Wave power Plant Master thesis, University of Limerick, 1994